DOI 10.1002/pmic.200800293 *Proteomics* 2009, *9,* 138–147

RESEARCH ARTICLE

Combining subproteome enrichment and Rubisco depletion enables identification of low abundance proteins differentially regulated during plant defense

Ivy Widjaja[1], Kai Naumann[1], Udo Roth[1], Noreen Wolf[1], David Mackey[2], Jeffery L. Dangl[3, 4, 5, 6], Dierk Scheel[1] and Justin Lee[1]*

[1] Leibniz Institute of Plant Biochemistry, Halle, Germany
[2] Department of Horticulture and Crop Science, The Ohio State University, Columbus, OH, USA
[3] Department of Biology, University of North Carolina, Chapel Hill, NC, USA
[4] Curriculum in Genetics and Molecular Biology, University of North Carolina, Chapel Hill, NC, USA
[5] Department of Microbiology and Immunology, University of North Carolina, Chapel Hill, NC, USA
[6] Carolina Center for Genome Sciences, University of North Carolina, Chapel Hill, NC, USA

Transgenic *Arabidopsis* conditionally expressing the bacterial *avrRpm1* type III effector under the control of a dexamethasone-responsive promoter were used for proteomics studies. This model system permits study of an individual effector without interference from additional bacterial components. Coupling of different prefractionation approaches to high resolution 2-DE facilitated the discovery of low abundance proteins – enabling the identification of proteins that have escaped detection in similar experiments. A total of 34 differentially regulated protein spots were identified. Four of these (a remorin, a protein phosphatase 2C (PP2C), an RNA-binding protein, and a C2-domain-containing protein) are potentially early signaling components in the interaction between AvrRpm1 and the cognate disease resistance gene product, resistance to *Pseudomonas syringae* pv. maculicola 1 (RPM1). For the remorin and RNA-binding protein, involvement of PTM and post-transcriptional regulation are implicated, respectively.

Received: April 2, 2008
Revised: July 15, 2008
Accepted: July 16, 2008

Keywords:
2-DE / *Arabidopsis thaliana* / AvrRpm1 / Lipid raft / Signaling

Correspondence: Dr. Justin Lee, Leibniz Institute of Plant Biochemistry, Weinberg 3, D-06120 Halle, Germany
E-mail: jlee@ipb-halle.de
Fax: +49-345-5582-1409

Abbreviations: ETI, effector-triggered immunity; **HR,** hypersensitive response; **LRR,** leucine-rich repeat; **Myros.AP,** myrosinase-associated protein; **NB,** nucleotide-binding; **PAL,** phenylalanine ammonia-lyase; **PAMP,** pathogen-associated molecular pattern; **PP2C,** protein phosphatase 2C; **RIN4,** RPM1-interacting protein 4; **RPM1,** resistance to *Pseudomonas syringae* pv. maculicola 1; **SB,** solubilization buffer

1 Introduction

Notwithstanding advances in LC-based approaches for automated gel-free separation and identification in complex samples [1, 2], 2-DE is still a proven strategy due to its resolution and quantitative reliability [3]. *Mycobacterium tuberculosis* proteome analysis revealed bias in the two methods – with better coverage for low or high molecular weight pro-

* Current address: Qiagen GmbH, Hilden, Germany.

teins by 2-DE or LC–MS/MS, respectively [4]. Despite the assertion that IEF-based 2-DE is unsuitable for analyzing membrane proteins, it covers hydrophobic proteins better than LC-based methods [4]. Moreover, the 2-DE-based approach can quantify the abundance of protein isoforms, such as differential PTMs, which is difficult with LC-based methods. Hence, complementary use of both techniques is advisable.

Current proteomics studies are often limited to identification of abundant targets [1, 5]. The identification of low abundance proteins is especially impeded by predominating proteins. For example, Rubisco (ribulose-1,5-bisphosphate carboxylase/oxygenase), the most abundant protein in green plant tissues, diminishes 2-DE resolution by limiting the loading capacity. Thus, Rubisco depletion and/or prefractionation targeting specific subcellular proteomes can reduce protein complexity and enhance detection of other proteins [6].

Plant immunity is multilayered, one form uses extracelullar surface receptors to recognize pathogen-associated molecular patterns (PAMPs), triggering defense responses resulting in the so-called PTI (PAMP-triggered immunity) [7, 8]. Some pathogens have developed virulence factors (*e.g.*, bacterial type III effectors) to suppress and overcome PTI, rendering the plants susceptible. Plants, in turn, evolved additional surveillance mechanism to recognize pathogen effectors, leading to effector-triggered immunity (ETI). ETI is activated by the so-called *R* (disease resistance) genes that encode polymorphic proteins, often featuring nucleotide-binding (NB) and leucine-rich repeat (LRR) domains. Specific NB–LRR proteins respond to the products of avirulence (*avr*) genes expressed by the pathogen and subsequently trigger ETI that often culminates in hypersensitive response (HR, a form of programmed cell death) [7].

Most studies of NB–LRR-mediated disease resistance rely on transcriptomics platforms or screening for mutants with altered levels of disease resistance [9–12]. Only a few proteomics studies exist that examine changes in *Arabidopsis* challenged with virulent and avirulent *P. syringae* strains. These reported changes in defense-related antioxidants, metabolic enzymes, and potentially phosphorylated proteins [13–15].

We performed a targeted proteomics approach to identify proteins involved in early signaling steps of ETI mediated by the resistance to *P. syringae* pv. maculicola 1(RPM1) NB–LRR protein [16]. A transgenic model system featuring conditional *avrRpm1* expression was used to identify proteins specifically involved in the AvrRpm1–RPM1 interaction without interference from additional bacterial components. We used 2-DE following subproteome enrichment and/or depletion of high abundance proteins to enhance the detection of low abundance protein changes during early phases of RPM1-mediated ETI. Systematic microsomal fractionation and Rubisco depletion facilitated detection of candidates with potential roles in early signaling, which escaped detection with proteomics based on total protein extracts.

2 Materials and methods

2.1 Plant growth and treatment

The Col-0 *Arabidopsis* lines used in these experiments expressed *avrRpm1* under the control of a dexamethasone-responsive promoter [17]. As a control, the same construct was expressed in the *rpm1–3* background (an allele of *RPM1* with a stop codon at amino acid 87) [16]. Four-week-old plants were sprayed with 20 μM dexamethasone in 0.0075% Silwet L-77 and harvested 2 and 6 h later.

2.2 Total protein extraction

Ground leaf material (500 mg) was extracted with 1.5 mL extraction buffer (5% glycerol, 5 mM EDTA, 0.1% β-mercaptoethanol, 100 mM HEPES-KOH, pH 7.5, 1% proteinase inhibitor cocktail) and centrifuged (10 min, 18 000 × *g*, 4°C). The supernatant was mixed with an equal volume of phenol and centrifuged (10 min, 7850 × *g*, 4°C). The lower phase was re-extracted twice with an equal volume of buffer (20 mM KCl, 10 mM EDTA, 0.4% β-mercaptoethanol, 100 mM Tris-HCl, pH 8.4) then centrifuged (10 min, 7850 × *g*, 4°C). The final lower phase was precipitated by adding five volumes of precipitation solution (100 mM CH_3COONH_4 in methanol) for at least 2 h at −20°C. After centrifugation (10 min, 7850 × *g*, 4°C), the protein pellet was consecutively rinsed with precipitation solution and washing solution (80% ethanol in 50 mM Tris-HCl, pH 7.5), and solubilized in 150 μL of SB (solubilization buffer: 7 M urea, 2 M thiourea, 50 mM DTT, 2% IPG buffer, 4% CHAPS, 0.4% SDS, 5 mM K_2CO_3).

2.3 Microsomal fraction extraction

Ground leaf material (2.5 g) was homogenized (2 × 30 s) in a Polytron (Kinematica) in 20 mL of extraction buffer I (100 mM NaCl, 20 mM DTT, 0.33 M sucrose, 0.1% protease inhibitor cocktail, 1 mM PMSF, 50 mM Tris, pH 8.0). The extract was cleared by filtration through Nylon Net Filters (Millipore) and centrifugation (20 min, 3000 × *g*, 4°C). The microsomal pellet obtained after centrifugation (2 h, 100 000 × *g*, 4°C) was extracted in 700 μL of extraction buffer II (100 mM NaCl, 20 mM DTT, 1% protease inhibitor cocktails, 0.1% Triton X-100, and 0.1% NP-40, 50 mM Tris, pH 9.6) by vortexing for 30 min at room temperature. Insoluble debris was removed by centrifugation (10 min, 20 000 × *g*, 4°C). The supernatant was mixed with an equal volume of phenol and processed as described for total protein extraction.

2.4 Rubisco depletion from total protein

Fractionation procedure to reduce Rubisco abundance was adapted from Kim *et al.* [18]. Ground leaf material (2 g) was extracted in 12 mL of extraction buffer (20 mM $MgCl_2$, 2% β-mercaptoethanol, 0.1% protease inhibitor cocktail, 1 mM

PMSF, 1% PVPP, 2% NP-40, 500 mM Tris-HCl, pH 8.3) and clarified as described above. The supernatant was mixed with 50% PEG solution to a final concentration of 10% PEG. After 30 min, the mixture was centrifuged (10 min, 1500 × *g*, 4°C) to obtain 10% PEG pellet. The remaining supernatant was adjusted to a final concentration of 20% PEG with 50% PEG solution, incubated for another 30 min and centrifuged (15 min, 12 000 × *g*, 4°C) to obtain 20% PEG pellet. The remaining supernatant was precipitated with acetone. All pellets were washed (ice-cold acetone with 0.07% β-mercaptoethanol) and solubilized in SB (250 μL).

2.5 Rubisco depletion from microsomal fraction

Ground leaf material (8 g) was subjected to microsomal fraction extraction. The microsomal pellet was extracted in 4 mL of buffer II containing magnesium and NP-40 (100 mM NaCl, 20 mM DTT, 20 mM $MgCl_2$, 0.1% protease inhibitor cocktails, 1 mM PMSF, 2% NP-40, 0.1% Triton X-100, 50 mM Tris, pH 9.6) and incubated for 30 min with shaking at room temperature. Insoluble debris was removed by centrifugation (15 min, 12 000 × *g*, 4°C) and the extract subjected to PEG precipitation as described above.

2.6 Rubisco depletion using Seppro® IgY-Rubisco spin column (Genway)

Protein (200 μg) was diluted with TBS buffer (final volume: 500 μL), subjected to immunocapture of Rubisco according to the manufacturer's instruction and precipitated using TCA/acetone. The pellet was washed thrice (ice-cold acetone, 0.07% β-mercaptoethanol), and solubilized in SB (30 μL).

2.7 2-DE

Protein concentration was determined using 2D-Quant Kit (GE Healthcare). Total protein (150 μg) was resuspended in 450 μL of rehydration buffer (8 M urea, 2% CHAPS, 2.8% DTT, 0.5% IPG buffer, 0.002% BPB) and centrifuged (5 min, 13 000 × *g*) to remove nonsoluble material. The samples were loaded onto 24 cm 4–7 IPG strip (GE Healthcare) and actively rehydrated (12 h, 50 V) using an IPGphor (GE Healthcare). IEF was performed with the program: 200 V (1 h), 500 V (1 h), 1000 V (1 h), gradient to 8000 V (1.5 h), and constant 8000 V for 72 kV·h. After focusing, the IPG strip was equilibrated for 15 min (room temperature) in equilibration buffer (6 M urea, 30% glycerol, 2% SDS, 50 mM Tris-HCl, pH 8.8) containing 1% DTT and a second time in buffer with 2.5% iodoacetamide. The second dimension separation on 12% PAGE (Ettan Dalt II system, GE Healthcare). The gels were silver-stained according to Blum *et al.* [19].

2.8 Image analysis

The silver-stained gels were scanned using ImageScanner (GE Healthcare) and analyzed using Proteomweaver (BioRad). After spot detection, gels were fully matched and normalized by determining normalization factors for all pairs of gels using a precision normalization algorithm. These were then used to calculate intensity factors for each gel, which brought the normalization factors as close to one as possible. To find upregulated or downregulated proteins, a filter was implemented to search for spots with regulation factors of $\geq$1.5 or $\leq$0.75 compared to the control. The resulting spots were subsequently analyzed statistically to fulfill significance of $p<0.05$ (Student's *t*-test). Only data reproducibly obtained in three independent biological replicates are considered.

2.9 Protein identification by MALDI-TOF/MS

Protein spots were excised from 2-DE gels and destained with an equal mixture of 30 mM potassium ferricyanide and 100 mM sodium thiosulfate, and dried in a SpeedVac (30 min). The dried gel plugs were swollen with 5 ng/μL trypsin solution in digestion buffer containing 10 mM ammonium bicarbonate and 5% ACN for 30 min on ice and digested (37°C, 4 h). The peptide fragments were extracted using extraction buffer containing 50% ACN and 0.1% TFA. The extract was spotted onto prestructured MALDI sample support (AnchorChip 384/600; Bruker) and mixed with 2,5-DHB (2,5-dihydroxybenzoic acid) as MALDI matrix. After crystallization the samples were analyzed on Bruker's REFLEX III using Reflecton mode. The MALDI-TOF spectrum was analyzed by FlexAnalysis 2.0 (Bruker) and internally calibrated using trypsin autolysis peaks. Protein identification by PMF was performed using MASCOT software, allowing one missed tryptic cleavage and partial oxidation of methionine as well as modification of cysteines to complete alkylation. The search was against the database from TAIR7 (The Arabidopsis Information Resource) and proteins with MOWSE scores over the cut-off of 57 ($p<0.05$) were considered identified.

2.10 Phosphopeptide enrichment and Nano-LC-MS/MS analysis of peptides

Tryptic peptides were dissolved in a 0.1% TFA solution and analyzed by LC-MS/MS consisting of a nano-LC (UltiMate3000, Dionex) and an IT mass spectrometer (HCTultra PTM Discovery System, Bruker Daltonik). Peptides were preconcentrated on a trap column and separated on a RP column (C18 PepMap 100, Dionex) with a flow of 240 nL/min (Gradient: 2 → 30% B in 30 min; A: 0.1% formic acid in H_2O, B: 0.1% formic acid in ACN), transferred to the nano-ESI source of the mass spectrometer and sequenced in CID, alternating CID/electron transfer dissociation (ETD) or neutral loss triggered CID/ETD mode. Full scan was performed in standard enhanced mode (400–1700 m/z) followed by CID and ETD fragmentation (MS/MS) of the selected precursor ions. After phosphopeptide enrichment using *PHOS-Select*™ Iron Affinity Gel (Sigma) the eluted fraction were analyzed by a data-dependent neutral loss experiment (MS^3, CID, and

ETD of the selected precursor ion) triggered by detecting a loss of 58, 49, 38.7, and 32.7 in the five most abundant MS^2 fragments during CID mode. Fluoranthene radical anion transfer was optimized by achieving an ICC of 500-600.000 (accumulation time of 2.0–3.0 ms) for an efficient ETD process. Processed mass spectra were searched against TAIR7 by using a MASCOT server (Version 2.2.04, Matrix Science).

2.11 RT-PCR

RNA was isolated using the TRIZOL method. After DNAse treatment, RT-PCR was performed using Ready-to-Go RT-PCR Beads (GE Healthcare). PCR amplifications were carried out with 50% of the cDNA products (from 100 ng total RNA) using the following primer pairs:

AtREM1.2: 5′-AAAAAGCAGGCTCCATGGCGGAGGAACAGAAGATAGC-3′, 5′-AGAAAGCTGGGTTGAAACATCCACAAGTTGC-3′, PP2C: 5′-CACCATGGCAGGCAGAGAGATTCTCC-3′, 5′-CTGGAACCTTACAACTATACAAGAAATG-3′, RNA-BP45: 5′-CACCATGATGCAGCAGCCACCACCCG-3′, 5′-CTTCTCGGAAAACTGAACGAATCC-3′; C2-domain protein: 5′-CACCATGTCGATGATGGCGGGTAT-3′, 5′-CTAGTATGGAGGAGGTGGGTATTG-3′); EF1α: 5′-TTGATCTGGTCAAGAGCCTCAAG-3′, 5′-TCACATCAACATTGTGGTCATTGGC-3′.

3 Results and discussion

3.1 Differentially regulated proteins during the interaction of AvrRpm1 and RPM1

To find proteins involved in early regulatory events during an AvrRpm1–RPM1 interaction, we compared changes in protein patterns of two isogenic *Arabidopsis* lines with the same dexamethasone-inducible *avrRpm1* transgene, but differing in the absence or presence of the *RPM1* gene [17, 20]. This transgenic system avoids the confounding effects of signaling *via* PAMPs and other type III effectors when using *avrRpm1*-expressing bacteria.

Two representative time points were chosen. The "early" sample was taken 2 h after dexamethasone treatment, shortly after *avrRpm1* mRNA was detectable (data not shown, see Fig. 1). The "late" sample was taken 6 h after dexamethasone treatment, when the HR, in the form of tissue collapse, was starting (Fig. 1). This timing of *avrRpm1* transcript appearance and HR development in the transgenic line is comparable to that following inoculation with *P. syringae* DC3000 containing *avrRpm1* (*Pto* DC3000(*avrRpm1*)), where *avrRpm1* transcripts were detectable 30–60 min after bacterial challenge and initial signs of tissue collapse occurred 5 h postchallenge [10].

The hypothetical expression profiles depicted in Fig. 1 served as the filtering basis in the image analysis (ProteomWeaver). Proteins involved in signaling may be transiently upregulated at an early time point (profile c), upregulated at early time points and maintained at a steady state (profile b), or continuously increasing (profile a, Fig. 1A). Secondary stress reactions are expected for upregulation at late time points (profile d). The reciprocal profiles might also be expected with protein downregulation during the response (Fig. 1B). Proteins were considered up- or downregulated if the spot intensities differed $\geq$1.5- or $\leq$0.75-fold from a preceding time point. Only changes with *p*-values less than 0.05 (Student's *t*-test) and reproduced in at least three independent biological experiments are reported.

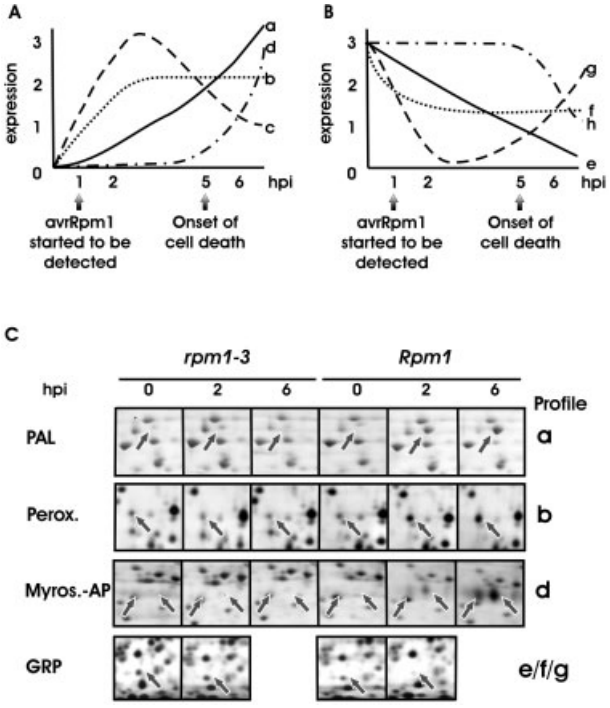

Figure 1. Hypothetical expression profiles of proteins involved in specific recognition events in plant–pathogen interactions. The definition of the time points are based on the onset of HR (late, 5 hpi) and the presumed initiation of defense shortly after *avrRpm1* mRNA expression is detectable (early, 1–2 hpi) (A) Proteins involved in signaling may be transiently upregulated early, *i.e.*, at 2 h (profile c), upregulated at early time points and maintained at a steady state (profile b) or continuously increasing (profile a). Secondary stress reactions are expected for upregulation at late time points (profile d). The expected reciprocal profiles for downregulated protein are shown in (B). (C) Selected examples of proteins of expression profiles a, b, and d are illustrated. (PAL, Perox, Myros.AP). The downregulated Glycine-rich protein (GRP) was subsequently found in fractionated samples, where only two time points were used; hence it could belong to expression profiles e, f, or g.

3.2 Differential regulation of proteins in total protein extract

For an initial global overview, total protein was analyzed. Our protocol for high resolution 2-DE enabled visualization of

~1500 protein spots in total extracts (Fig. S1 of Supporting Information and Fig. 2), which is almost twice the number of spots resolved in similar experiments with *Arabidopsis* leaves [13, 14]. Figure 1C shows selected examples with expression profiles a, b, and d; no proteins with transient expression (profile c) or downregulated proteins were found at this stage. Sixteen candidates with increased expression were picked and identified by MS (first three columns in Table 1; details of statistical evaluation, expression levels, and protein identification are in Table S1 of Supporting Information). These include proteins with putative functions in general metabolism or defense; some were known from previous studies [13, 14]. Signaling proteins, presumably of low abundance, were not found.

3.3 Differential regulation of proteins in microsomal protein extract

One strategy to enhance the sensitivity of 2-DE is to analyze subproteomes. Microsomal proteins were chosen since several components of AvrRpm1–RPM1 signaling are membrane associated. RPM1 is a peripheral plasma membrane protein [21] and AvrRpm1 is membrane-localized *via* N-terminal myristoylation [22]. RPM1-interacting protein 4 (RIN4) and NDR1, proteins required for RPM1 function, are also localized to membranes *via* C-terminal acylation or glycosylphosphatidyl-inositol anchoring, respectively [17, 23, 24].

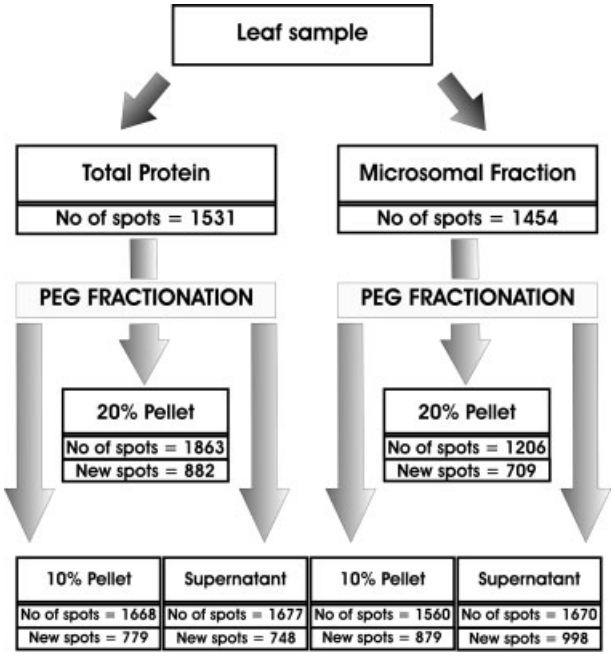

Figure 2. Scheme of the fractionation steps applied to the protein samples. The number of protein spots and the number of new spots (as compared to the nonfractionated sample) from each fraction are indicated. Representative corresponding gels are in Figs. S1 and S2 of Supporting Information.

About 1500 microsomal proteins were resolved (Fig. 2 and Fig. S2 of Supporting Information). However, both subunits of Rubisco were more abundant in microsomal than in total protein fractions (*cf.* Figs. S1 and S2 of Supporting Information). Some of the differentially regulated proteins in the microsomal fraction overlapped with soluble proteins identified in total protein extracts including phenylalanine ammonia-lyase (PAL) and glutathione transferase (GST) (Table 1). Thus, certain abundant proteins, including Rubisco, were likely trapped during microsome preparation.

The results from microsomal fraction analysis confirmed the findings from total protein and added two candidates – myrosinase-associated protein (Myros.AP, At3g14210) and a member of the remorin family, AtREM1.2 (At3g61260) [25]. Each of these proteins was present as two isoforms. Both Myros.AP isoforms and only one AtREM1.2 isoform were upregulated (Table 1). The high amounts of Rubisco in these fractions may account for our ability to identify only one putative signaling protein, AtREM1.2. Thus, we sought to deplete Rubisco before further analysis.

3.4 Identification of candidates after Rubisco depletion

Rubisco can be depleted from plant tissue extracts using differential precipitation by PEG [18, 26, 27]. We adapted the protocol in ref. [18] to deplete Rubisco from total and microsomal proteins. Rubisco is enriched in the 20% PEG pellet, strongly reduced in the 10% PEG pellet and almost absent from the 20% PEG supernatant (Figs S1 and S2). Therefore, the 10% PEG pellet and 20% PEG supernatant fractions were analyzed by 2-DE. Since the number of gels for each sample escalates after fractionation, analysis was restricted to the 2 h time point.

The complexity of total and microsomal proteins is revealed by the increment in proteins detected after fractionation (~700–1000 new spots *per* fraction, Fig. 2). When a composite gel of the Rubisco-depleted fractions (*i.e.*, 10% PEG pellet and 20% PEG supernatant fractions) was compared to the corresponding unfractionated sample, many new or spots with increased abundance were detected (marked as crosses in Figs. S1A and S2A of Supporting Information). Thus, the proteome coverage is enhanced through fractionation and Rubisco depletion.

After Rubisco depletion from total protein, new proteins were found at the early time point. Only one candidate (PSII-P) from Rubisco-depleted total protein overlapped with candidates from total protein. Proteins involved in metabolism and photosynthesis are still predominant (Table 1), including three new metabolic proteins that were not observed prior to fractionation. New candidates potentially involved in signaling include a protein phosphatase 2C (PP2C, At2g20630) and an RNA-binding protein (At1g11650). A third isoform of AtREM1.2 was detected, but levels of this isoform were constant. Two proteins with unknown functions (At5g48930 and At4g39260) were downregulated (Table 1 and Fig. 1C).

Table 1. Classification of differentially expressed proteins according to biological function and expression pattern in different fractions

		T[a]			MF[b]			TPEG[c]		MFPEG[d]	
		0[e]	2[f]	6[g]	0	2	6	0	2	0	2 (h)
Defense											
1	Phenylalanine ammonia-lyase 2, (At3g53260)	+	++	+++	+	++	++				
2	Peroxiredoxin type 2, putative, (At3g52960)/Prx IIE	+	++	++							
3	Glutath. transferase GSTF6[1], (At1g02930)	+	+	++							
4	Glutath. transferase GSTF6[2], (At1g02930)	+	+	++							
5	Glutath. transferase GSTF7, (At1g02920)	+	++	+++							
6	Myrosinase-assoc. prot. like[1], (At3g14210)				−	−	+				
7	Myrosinase-assoc. prot. like[2], (At3g14210)				−	−	+				
RNA processing											
1	29 kDa, ribonucleoprot., put. RNA-binding prot., chloropl., (At2g37220)	+	+	++							
2	Similar to RNA-binding prot. 45, (At1g11650)							−	+		
Metabolism and photosynthesis											
1	RBCL[1]	+	+	++	+	+	++				
2	RBCL[2]				+	+	++				
3	RBCL[3]	+	+	++							
4	RBCL[4]				−	−	+				
5	RBCL[5]				−	−	+				
6	Carbonic anhydrase, chloropl. precursor, (At3g01500)	+	+	++							
7	O_2-evolv. complex subunit 33 kDa, (At5g66570)/OEC33	+	++	+++							
8	Similar to malate dehydrogenase, (At5g09660)	+	+	++							
9	O_2-evolv. complex subunit 23 kDa, (At1g06680)/PSII-P	+	+	++				−	+		
10	Malic enzyme/AtNADP_ME2, (At5g11670)	+	++	+++							
11	Glutamine synthase, chloroplastic, (At5g35630)	+	++	++							
12	Serine hydroxymethyltransf. 1, (At4g37930)	−	−	+							
13	Rubisco activase, (At2g39730)							−	+		
14	O_2-evolv. complex subunit 16 kDa, (At4g05180)/PSII-Q							−	+		
15	Oxidoreductase, (At5g05600)							−	+		
Signaling											
1	AtREM1.2[1], (At3g61260)				+	+	+	+	+	+	+
2	AtREM1.2[2], (At3g61260)				+	++	++	+	++	+	++
3	AtREM1.2[3], (At3g61260)							+	+	+	+
4	AtREM1.2[4], (At3g61260)									+	++
5	AtREM1.2[5], (At3g61260)									−	+
6	Prot. phosphatase 2C, (At2g20630)							+	++	+	++
7	C2-domain-containing prot., (At4g34150)									+	++
Unknown functions											
1	S locus F-box-related, (At1g12870)	+	+	++							
2	Hydroxycinnam.-CoA shikimate/quinate hydroxycinnam. transferase, (At5g48930)							++	+		
3	Glycine-rich prot., (At4g39260)							++	+		
	Number of proteins	16			9			11		7	

Superscript numbers 1–5 beside the protein ID refer to protein isoforms observed on 2-DE gels.

a) Total protein.
b) Microsomal protein.
c) Rubisco-depleted total protein.
d) Rubisco-depleted microsomal protein.
e) 0 h after dexamethasone treatment.
f) 2 h after dexamethasone treatment.
g) 6 h after dexamethasone treatment.

The absolute number of candidates identified from the Rubisco-depleted microsomal protein fraction, was limited, but all candidates were potentially involved in signaling (Table 1). This underscores the effectiveness of Rubisco depletion and fractionation to reveal low abundance signaling proteins. Beside PP2C (At2g20630) and AtREM1.2, a C2-domain-containing protein (At4g34150) and two more AtREM1.2 isoforms were identified.

3.5 Comparison to commercial Rubisco-removal spin columns

We compared our Rubisco-depletion strategy to commercial Seppro IgY-Rubisco spin columns, which very effectively removed Rubisco (Fig. S3 of Supporting Information). Although the overall protein patterns are similar between the two methods (Fig. S3C of Supporting Information), abundant proteins in the Seppro sample still predominate and impede detection of low abundance proteins. The three candidates detected in Rubisco-depleted total proteins after PEG fractionation (RNA-binding protein 45, AtREM1.2, and PP2C) were not visible in the Seppro sample. Moreover, frequent contamination with IgY fragments interfered with PMF-based identification. Hence, the more labor-intensive Rubisco depletion *via* PEG fractionation is superior to the antibody-based depletion.

3.6 Potential functions/roles of the candidates

Metabolism-related proteins comprise the largest upregulated group (Table 1). Increased demand for energy and biosynthetic capacity may result from NADPH-consuming reactions activated during defense. Upregulation of enzymes involved in NADPH production (At5g09660, At5g11670) may contribute to replenishing NADPH. NADPH also acts as electron donor to oxygen leading to the formation of ROS during the oxidative burst [28]. Upregulation of photosystem II components seen here (Table 1) was also described in ref. [14] and may serve as an additional source of ROS. In general, most of the proteins involved in metabolism started to accumulate early and remained at steady or increased levels until the onset of HR. De Torres *et al.* [10] found genes involved in metabolic processes to be transcriptionally upregulated shortly (0.5–1 h) after infection. Our identification of early upregulation and maintenance of metabolic proteins supports a role for increased energy supply during defense.

The second largest group of upregulated proteins encompasses defense-related proteins (Table 1). Expression of GSTF7, peroxiredoxin (Perox), and PAL increased early and continued until HR formation, whereas GSTF6 and Myros.AP were upregulated at the occurrence of HR. PAL catalyzes the conversion of phenylalanine to *trans*-cinnamic acid, the first committed step of phenylpropanoid biosynthesis leading to diverse plant metabolites, some of which are involved in plant defense reactions [29]. Truman *et al.* [30] detected the accumulation of PAL transcripts systemically 4 h after infiltration with *Pto* DC3000(*avrRpm1*), which is in agreement with our finding of early upregulation of PAL. The upregulation of redox enzymes before, and concomitantly with, HR may function to protect neighboring cells from damage by toxic ROS produced during the oxidative burst [31]. Conceivably, this may restrict the extent of cell death to a localized area in a typical HR initiated by avirulent pathogens.

We considered four candidate proteins to have potential early signaling roles: RNA-binding protein 45 (At1g11650), a PP2C (At2g20630), a C2-domain-containing protein (At4g34150), and AtREM1.2 (At3g61260). All of them fulfill our criteria of early upregulation (Fig. 3A). AtREM1.2 and the C2-domain-containing protein were further upregulated until HR initiation (not shown).

While RNA-binding proteins are generally not ascribed with signaling roles, they may be interesting since involvement in plant immunity has been implicated. For instance, expression of an RNA-binding protein is regulated during TMV-induced HR [32]. Recently, five RNA-binding proteins were found to be ADP-ribosylated by the type III effector, HopU1, and a null mutant of one of them, *grp7*, was more

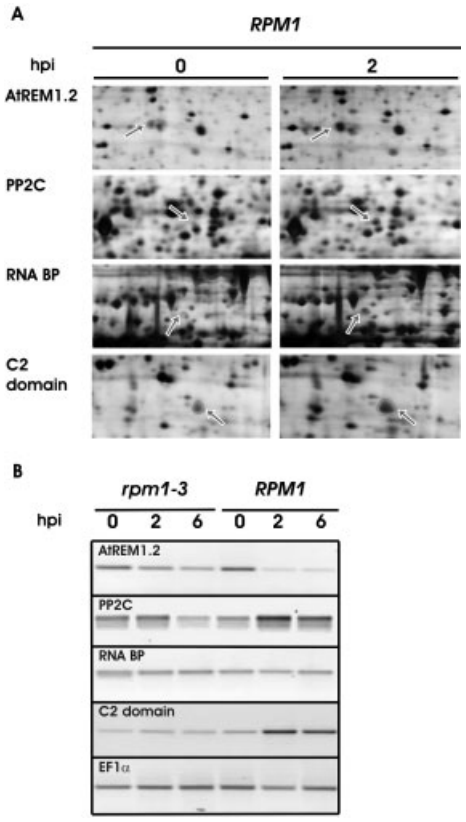

Figure 3. Comparison of the protein and transcript levels of four candidate proteins upregulated at the early time point. (A) Panels of selected regions of 2-DE gels showing protein spots (indicated by arrows) before and 2 h after dexamethasone treatment. (B) Semiquantitative RT-PCR analysis of the mRNA levels, with EF1α as a constitutive control, is shown.

susceptible to *P. syringae* [33]. Moreover, one of these ADP-ribosylated RNA-binding proteins, At2g37220, was also found to be upregulated in our total extract at 6 h (Table 1).

During AvrRpm1–RPM1 interaction, RIN4 is rapidly hyper-phosphorylated [17], but the kinases or phosphatases involved are unknown. Regulation of protein phosphorylation states by PP2Cs has been implicated in plant stress responses – especially in the ABA and MAPK pathways that regulate osmotic stress response and disease resistance [34]. The C2-domain is a conserved module that binds phospholipids in a calcium-dependent manner [35] or coordinates recruitment of the C2-domain-containing proteins to specific membrane compartments [36]. The timing of the PP2C (At2g20630) and C2-domain-containing protein (At4g34150) upregulation coincides with RIN4 phosphorylation. Furthermore, their presence in the microsomal membrane fraction indicates that they may be properly localized to regulate phosphorylation of RIN4.

AtREM1.2 was detected reproducibly in the microsomal fraction, as well as in Rubisco-depleted total and microsomal proteins. It appeared in several differentially expressed isoforms that indicate possible PTM. Remorins are plant-specific plasma membrane lipid-raft-associated proteins of unknown function [37, 38]. Their involvement in defense was first uncovered in potato, where remorin is phosphorylated *in vitro* upon oligogalacturonic acid addition to potato plasma membrane preparations [39]. Due to the characteristic enrichment of sterols and sphingolipids in lipid raft microdomains, lipid rafts might recruit specific membrane proteins, and exclude others, thus facilitating protein–protein interaction or modulating protein complexes. MLO, a protein required for the entry of powdery mildew into leaf epidermal cells, was found to be recruited to pathogen entry sites and may indicate hijacking of lipid raft function for pathogen entry [37].

3.7 Some candidates are post-transcriptionally or post-translationally regulated

Transcript levels of PP2C and C2-domain-containing protein were elevated in an RPM1-dependent manner (Fig. 3B), which correlated to upregulation of their protein levels (Fig. 3A). AtREM1.2, however, showed decreased transcript levels, while the putative RNA-binding protein transcript levels remained constant during the analyzed time course (Fig. 3B). Thus, these proteins are regulated post-transcriptionally and would have been missed in mRNA-based studies [9, 10].

Two isoforms of AtREM1.2 were initially identified in the microsomal fraction – both with very low spot intensities (Fig. 4B). As more extensive fractionation was performed, more AtREM1.2 isoforms were uncovered. In Rubisco-depleted total protein, three isoforms were identified with higher spot intensities than in the nondepleted sample (Fig. 4C). Changes were detected in the abundance of three out of five AtREM1.2 isoforms in Rubisco-depleted microsomal protein (Fig. 4D). Since the observed changes were *RPM1* dependent, we can exclude that the isoforms are artifacts of the fractionation procedure.

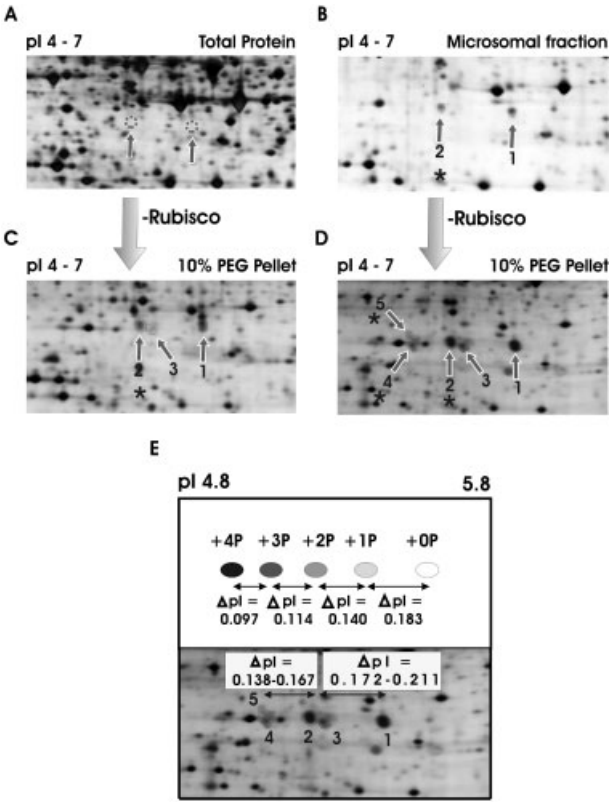

Figure 4. Increasing numbers of remorin isoforms were recovered after fractionation. Remorin isoforms were not detected in total protein but their positions relative to other proteins are indicated (A). Two isoforms of remorin were detected in the microsomal protein fraction (B). After Rubisco depletion from total protein extract, a third isoform was detected (10% PEG pellet, C). In the Rubisco-depleted microsomal protein fraction, a total of five isoforms were detectable (10% PEG pellet, D). Asterisks mark the upregulated isoforms. (E) Theoretical pattern of phosphorylated remorin on 2-DE gels predicted by ProMoST matches the observed pattern. Selected region of the 2-DE gel (as shown in D) was aligned to the ProMoST prediction of single or multiple phosphorylation effects on the Δp*I*. The p*I* shift between isoform 1 and isoforms 2/3 fits the theoretical value for single phosphorylation, while the p*I* shift between isoforms 2/3 and 4/5 fits the theoretical value for double phosphorylation. The disparity between theoretical and observed Δp*I* shifts might be due to the inaccuracy in p*I* calibration, which was determined by the ProteomWeaver software on the basis of the p*I* range of the IPG strips used.

The shift toward acidic p*I* indicated possible phosphorylations of the isoforms. The p*I* observed on 2-DE gels matched the theoretical phosphorylation patterns for single and dual-phosphorylation (Fig. 4E), as calculated by the Protein Modification Screening Tool (ProMoST) [40]. Other modifications between isoforms 4 and 5, as well as 2 and 3, may additionally exist since there are minor migration differences

(in the second dimension of 2-DE) (Fig. 4E). λ-Phosphatase treatment reduced the intensities of spots 2, 4, and 5, suggesting these isoforms are likely phosphorylated (Fig. 5A). For verification, the spots 1–3 were collected individually from eight separate silver-stained gels and subjected to nano-LC-MS/MS measurement, which confirmed their identity as AtREM1.2 (Fig. 5B and Table S2 of Supporting Information). Phosphopeptides were enriched by IMAC and subjected to analysis in the CID, alternating CID/ETD or neutral loss triggered CID/ETD mode but no phosphopeptides could be identified. This highlights the low abundance of these AtREM1.2 isoforms and emphasizes the sensitivity of our procedure for detecting novel low abundant targets.

4 Concluding remarks

We used targeted proteomics that combines microsomal enrichment and Rubisco depletion to find proteins involved in early AvrRpm1–RPM1-mediated signaling and identified four candidate proteins (RNA-binding protein 45, AtREM1.2, PP2C, and C2-domain-containing protein). Comparable proteomics experiments with bacteria-challenged plants [13–15] did not reveal the candidates described here, probably because fractionation enhances detection of less abundant proteins and our 2-DE provides higher resolution (~1500–1700 compared to ~800 protein spots in [14]). Clearly, our fractionation strategy is not fully exploited since small (<15 kD) or large (>100 kD) proteins are not covered by our gel system. Future analysis with suitable separation techniques (*e.g.*, tricine-gels for small peptides or shotgun LC-MS/MS) should further enhance the resolution. Since post-transcriptional/translational regulation is implicated for two candidates (Fig. 3), these would have been overlooked by mRNA analysis. In particular, we detected potential phospho-isoforms of remorin, which were differentially regulated during the AvrRpm1–RPM1 interaction. Overall, our extensive fractionation strategy enabled us to find novel low abundance candidates for further detailed functional studies, which are currently ongoing.

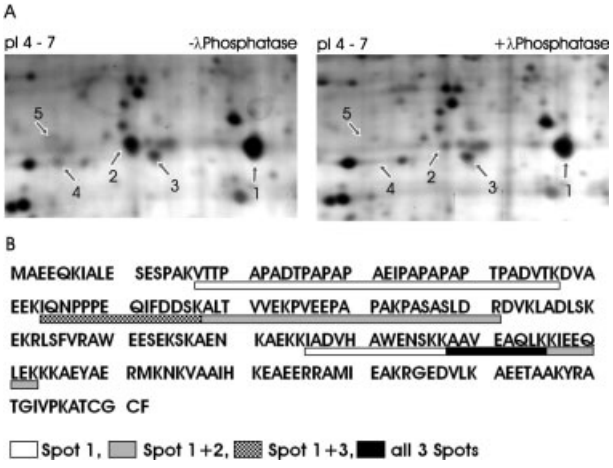

Figure 5. (A) Phosphatase treatment reduces the intensity of the remorin isoforms 2, 4, and 5. The 10% PEG-fractionated microsomal proteins were treated with λ-phosphatase (Upstate Cell Signaling, for 20 min, 30°C.) and analyzed by 2-DE. Spots 4/5 are only weakly expressed in this sample. (B) Nano-LC-MS/MS analysis confirmed Spots 1–3 to be AtREM1.2. Each spot was pooled from eight gels for MS/MS analysis. The peptides identified and their recoveries in individual AtREM1.2 isoforms are indicated. (Details are in Table S2 of Supporting Information).

This work was supported by grants to D. S. (BMBF, grant number 0312277I, GABI Arabidopsis Verbund III), to J. L. D. (NSF, Arabidopsis 2010), and to D. M. (NSF, grant number MCB-0718882). I. W. thanks Vincentius A. Halim for fruitful discussions and support throughout the research.

The authors have declared no conflict of interest.

5 References

[1] Patterson, S. D., Aebersold, R. H., Proteomics: The first decade and beyond. *Nat. Genet.* 2003, *33* 311–323.

[2] Hunt, D. F., Yates, J. R., III, Shabanowitz, J., Winston, S. *et al.*, Protein sequencing by tandem mass spectrometry. *Proc. Natl. Acad. Sci. USA* 1986, *83*, 6233–6237.

[3] Kabuyama, Y., Resing, K. A., Ahn, N. G., Applying proteomics to signaling networks. *Curr. Opin. Genet. Dev.* 2004, *14*, 492–498.

[4] Schmidt, F., Donahoe, S., Hagens, K., Mattow, J. *et al.*, Complementary analysis of the *Mycobacterium tuberculosis* proteome by two-dimensional electrophoresis and isotope-coded affinity Tag technology. *Mol. Cell. Proteomics* 2004, *3*, 24–42.

[5] Gorg, A., Weiss, W., Dunn, M. J., Current two-dimensional electrophoresis technology for proteomics. *Proteomics* 2004, *4*, 3665–3685.

[6] Rose, J. K., Bashir, S., Giovannoni, J. J., Jahn, M. M. *et al.*, Tackling the plant proteome: Practical approaches, hurdles and experimental tools. *Plant J.* 2004, *39*, 715–733.

[7] Jones, J. D., Dangl, J. L., The plant immune system. *Nature* 2006, *444*, 323–329.

[8] Chisholm, S. T., Coaker, G., Day, B., Staskawicz, B. J., Host-microbe interactions: Shaping the evolution of the plant immune response. *Cell* 2006, *124*, 803–814.

[9] Truman, W., de Zabala, M. T., Grant, M., Type III effectors orchestrate a complex interplay between transcriptional networks to modify basal defence responses during pathogenesis and resistance. *Plant J.* 2006, *46*, 14–33.

[10] de Torres, M., Sanchez, P., Fernandez-Delmond, I., Grant, M., Expression profiling of the host response to bacterial infection: The transition from basal to induced defence responses in RPM1-mediated resistance. *Plant J.* 2003, *33*, 665–676.

[11] Tao, Y., Xie, Z., Chen, W., Glazebrook, J. *et al.*, Quantitative nature of *Arabidopsis* responses during compatible and incompatible interactions with the bacterial pathogen *Pseudomonas syringae*. *Plant Cell* 2003, *15*, 317–330.

[12] Tornero, P., Chao, R. A., Luthin, W. N., Goff, S. A. *et al.*, Large-scale structure-function analysis of the *Arabidopsis* RPM1 disease resistance protein. *Plant Cell* 2002, *14*, 435–450.

[13] Jones, A. M., Thomas, V., Truman, B., Lilley, K. *et al.*, Specific changes in the *Arabidopsis* proteome in response to bacterial challenge: Differentiating basal and R-gene mediated resistance. *Phytochemistry* 2004, *65*, 1805–1816.

[14] Jones, A. M., Thomas, V., Bennett, M. H., Mansfield, J. *et al.*, Modifications to the *Arabidopsis* defense proteome occur prior to significant transcriptional change in response to inoculation with *Pseudomonas syringae*. *Plant Physiol.* 2006, *142*, 1603–1620.

[15] Jones, A. M., Bennett, M. H., Mansfield, J. W., Grant, M., Analysis of the defence phosphoproteome of *Arabidopsis thaliana* using differential mass tagging. *Proteomics* 2006, *6*, 4155–4165.

[16] Grant, M. R., Godiard, L., Straube, E., Ashfield, T. *et al.*, Structure of the *Arabidopsis* RPM1 gene enabling dual specificity disease resistance. *Science* 1995, *269*, 843–846.

[17] Mackey, D., Holt, B. F., III, Wiig, A., Dangl, J. L., RIN4 interacts with *Pseudomonas syringae* type III effector molecules and is required for RPM1-mediated resistance in *Arabidopsis*. *Cell* 2002, *108*, 743–754.

[18] Kim, S. T., Cho, K. S., Jang, Y. S., Kang, K. Y., Two-dimensional electrophoretic analysis of rice proteins by polyethylene glycol fractionation for protein arrays. *Electrophoresis* 2001, *22*, 2103–2109.

[19] Blum, H., Beier, H., Gross, H. J., Improved silver staining of plant proteins, RNA, and DNA in polyacrylamide gels. *Electrophoresis* 1987, *8*, 93–99.

[20] Andersson, M. X., Kourtchenko, O., Dangl, J. L., Mackey, D. *et al.*, Phospholipase-dependent signaling during the AvrRpm1- and AvrRpt2-induced disease resistance responses in *Arabidopsis thaliana*. *Plant J.* 2006, *47*, 947–959.

[21] Boyes, D. C., Nam, J., Dangl, J. L., The Arabidopsis thaliana RPM1 disease resistance gene product is a peripheral plasma membrane protein that is degraded coincident with the hypersensitive response. *Proc. Natl. Acad. Sci. USA* 1998, *95*, 15849–15854.

[22] Nimchuk, Z., Marois, E., Kjemtrup, S., Leister, R. T. *et al.*, Eukaryotic fatty acylation drives plasma membrane targeting and enhances function of several type III effector proteins from *Pseudomonas syringae*. *Cell* 2000, *101*, 353–363.

[23] Kim, H. S., Desveaux, D., Singer, A. U., Patel, P. *et al.*, The *Pseudomonas syringae* effector AvrRpt2 cleaves its C-terminally acylated target, RIN4, from *Arabidopsis* membranes to block RPM1 activation. *Proc. Natl. Acad. Sci. USA* 2005, *102*, 6496–6501.

[24] Coppinger, P., Repetti, P. P., Day, B., Dahlbeck, D. *et al.*, Overexpression of the plasma membrane-localized NDR1 protein results in enhanced bacterial disease resistance in *Arabidopsis thaliana*. *Plant J.* 2004, *40*, 225–237.

[25] Raffaele, S., Mongrand, S., Gamas, P., Niebel, A. *et al.*, Genome-wide annotation of remorins, a plant-specific protein family: Evolutionary and functional perspectives. *Plant Physiol.* 2007, *145*, 593–600.

[26] Lee, D. G., Ahsan, N., Lee, S. H., Kang, K. Y. *et al.*, A proteomic approach in analyzing heat-responsive proteins in rice leaves. *Proteomics* 2007, *7*, 3369–3383.

[27] Xi, J. H., Wang, X., Li, S. Y., Zhou, X. *et al.*, Polyethylene glycol fractionation improved detection of low-abundant proteins by two-dimensional electrophoresis analysis of plant proteome. *Phytochemistry* 2006, *67*, 2341–2348.

[28] Pugin, A., Frachisse, J. M., Tavernier, E., Bligny, R. *et al.*, Early events induced by the elicitor cryptogein in tobacco cells: Involvement of a plasma membrane NADPH Oxidase and activation of glycolysis and the pentose phosphate pathway. *Plant Cell* 1997, *9*, 2077–2091.

[29] Hahlbrock, K., Scheel, D., Physiology and molecular biology of phenylpropanoid metabolism. *Annu. Rev. Plant Physiol. Plant Mol. Biol.* 1989, *40*, 347–369.

[30] Truman, W., Bennett, M. H., Kubigsteltig, I., Turnbull, C. *et al.*, *Arabidopsis* systemic immunity uses conserved defense signaling pathways and is mediated by jasmonates. *Proc. Natl. Acad. Sci. USA* 2007, *104*, 1075–1080.

[31] Sutherland, M. W., The generation of oxygen radicals during host plant responses to infection. *Physiol. Mol. Plant Pathol.* 1991, *39*, 79–93.

[32] Naqvi, S. M., Park, K. S., Yi, S. Y., Lee, H. W. *et al.*, A glycine-rich RNA-binding protein gene is differentially expressed during acute hypersensitive response following Tobacco Mosaic Virus infection in tobacco. *Plant Mol. Biol.* 1998, *37*, 571–576.

[33] Fu, Z. Q., Guo, M., Jeong, B. R., Tian, F. *et al.*, A type III effector ADP-ribosylates RNA-binding proteins and quells plant immunity. *Nature* 2007, *447*, 284–288.

[34] Schweighofer, A., Hirt, H., Meskiene, I., Plant PP2C phosphatases: Emerging functions in stress signaling. *Trends Plant Sci.* 2004, *9*, 236–243.

[35] Newton, A. C., Johnson, J. E., Protein kinase C: A paradigm for regulation of protein function by two membrane-targeting modules. *Biochim. Biophys. Acta* 1998, *1376*, 155–172.

[36] Mellor, H., Parker, P. J., The extended protein kinase C superfamily. *Biochem. J.* 1998, *332*, 281–292.

[37] Bhat, R. A., Panstruga, R., Lipid rafts in plants. *Planta* 2005, *223*, 5–19.

[38] Morel, J., Claverol, S., Mongrand, S., Furt, F. *et al.*, Proteomics of plant detergent-resistant membranes. *Mol. Cell Proteomics* 2006, *5*, 1396–1411.

[39] Reymond, P., Kunz, B., Paul-Pletzer, K., Grimm, R. *et al.*, Cloning of a cDNA encoding a plasma membrane-associated, uronide binding phosphoprotein with physical properties similar to viral movement proteins. *Plant Cell* 1996, *8*, 2265–2276.

[40] Halligan, B. D., Ruotti, V., Jin, W., Laffoon, S. *et al.*, ProMoST (Protein Modification Screening Tool): A web-based tool for mapping protein modifications on two-dimensional gels. *Nucleic Acids Res.* 2004, *32*, W638–W644.

